Partially slotted silicon ring resonator covered with electro-optical polymer

Steglich, Patrick, Mai, Christian, Stolarek, David, Lischke, Stefan, Kupijai, Sebastian, et al.

Patrick Steglich, Christian Mai, David Stolarek, Stefan Lischke, Sebastian Kupijai, Claus Villringer, Silvio Pulwer, Friedhelm Heinrich, Joachim Bauer, Stefan Meister, Dieter Knoll, Mauro Casalboni, Sigurd Schrader, "Partially slotted silicon ring resonator covered with electro-optical polymer," Proc. SPIE 9891, Silicon Photonics and Photonic Integrated Circuits V, 98910R (13 May 2016); doi: 10.1117/12.2217725

SPIE.

Event: SPIE Photonics Europe, 2016, Brussels, Belgium

Best Student Paper Award

Partially slotted silicon ring resonator covered with electro-optical polymer

Patrick Steglich[a,b,*], Christian Mai[c], David Stolarek[c], Stefan Lischke[c], Sebastian Kupijai[d], Claus Villringer[a,b], Silvio Pulwer[a,b], Friedhelm Heinrich[a], Joachim Bauer[a], Stefan Meister[d], Dieter Knoll[c], Mauro Casalboni[b], and Sigurd Schrader[a]

[a]University of Applied Sciences Wildau, Hochschulring 1, 15745 Wildau, Germany
[b]University of Rome Tor Vergata, Via Orazio Raimondo 18, 00133 Rome, Italy
[c]IHP, Im Technologiepark 25, 15236 Frankfurt(Oder), Germany
[d]Technical University Berlin, Straße des 17. Juni 135, 10623 Berlin, Germany

ABSTRACT

In this work, we present for the first time a partially slotted silicon ring resonator (PSRR) covered with an electro-optical polymer (Poly[(methyl methacrylate)-co-(Disperse Red 1 acrylate)]). The PSRR takes advantage of both a highly efficient vertical slot waveguide based phase shifter and a low loss strip waveguide in a single ring. The device is realized on 200 mm silicon-on-insulator wafers using 248 nm DUV lithography and covered with the electro-optic polymer in a post process. This silicon-organic hybrid ring resonator has a small footprint, high optical quality factor, and high DC device tunability. A quality factor of up to 10^5 and a DC device tunability of about 700 pm/V is experimentally demonstrated in the wavelength range of 1540 nm to 1590 nm. Further, we compare our results with state-of-the-art silicon-organic hybrid devices by determining the poling efficiency. It is demonstrated that the active PSRR is a promising candidate for efficient optical switches and tunable filters.

Keywords: ring resonator, silicon photonics, slot waveguides, silicon-organic hybrid

1. INTRODUCTION

Driven by substantial research investments the integration of silicon based photonic devices on silicon-on-insulator substrates has reached a degree of maturity that already permits industrial adoption. However, silicon has a lack of linear electro-optical (EO) coefficient and therefore linear tunable filter and modulators using advanced modulation formats like quadrature phase-shift keying (QPSK) and 16-state quadrature amplitude modulation (16QAM) are difficult to realize.[1] During the last decade a different approach based on silicon slot waveguides has been proposed[2] and experimentally demonstrated to be suitable as optical phase shifter.[3,4] Infiltration of the interior of the slot waveguide with an EO polymer allows the use of the linear EO effect (Pockels effect). However, slot waveguide phase shifters suffer from relatively high losses mainly caused by sidewall roughness.[5] As a consequence, slot waveguide ring resonators have typically small optical quality factors (Q-factors).[4,6,7] To overcome this deficiency we have recently proposed a novel ring resonator concept where the ring is only partially slotted.[8] This partially slotted ring resonator (PSRR) combines an efficient slot waveguide phase shifter with a low loss and strongly guiding silicon strip waveguide in a single ring resonator. Here we demonstrate for the first time a PSRR covered by an active EO polymer to show the potential of the concept for optical tunable filters with high DC device tunability.

*E-mail: patrick.steglich@th-wildau.de

Silicon Photonics and Photonic Integrated Circuits V, edited by Laurent Vivien, Lorenzo Pavesi, Stefano Pelli,
Proc. of SPIE Vol. 9891, 98910R · © 2016 SPIE · CCC code: 0277-786X/16/$18 · doi: 10.1117/12.2217725

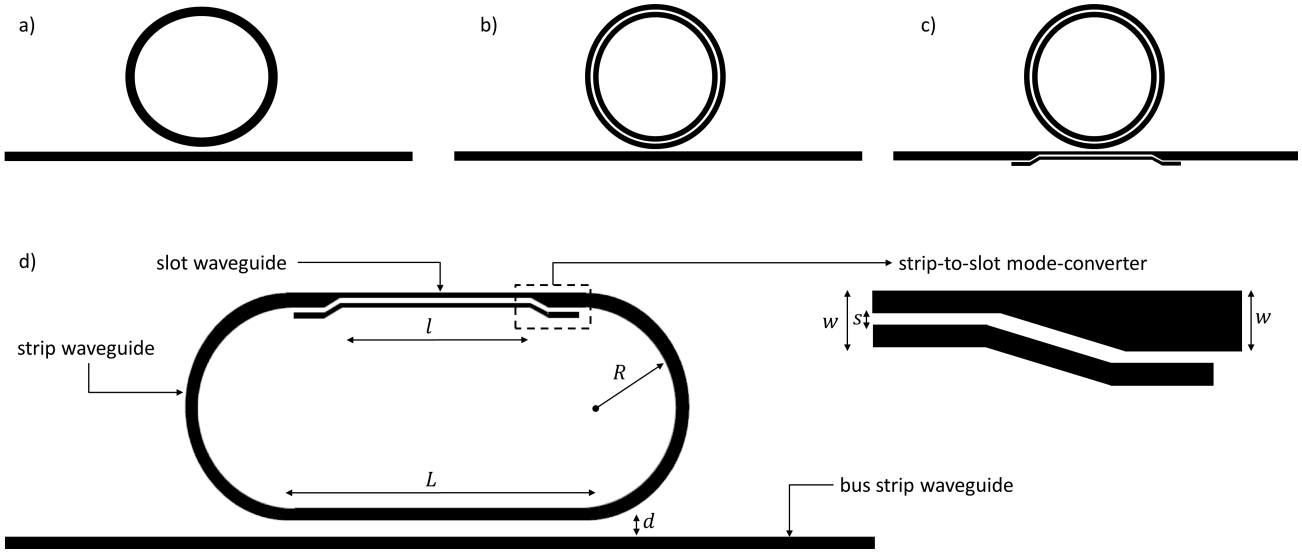

Figure 1. Schematics of different ring resonator concepts: a) Common silicon strip waveguide ring resonator. b) Fully slotted ring resonator with strip waveguide bus. c) Fully slotted ring resonator with slot waveguide bus. d) Partially slotted ring resonator with strip-to-slot mode-converter.

2. DEVICE DESIGN AND FABRICATION

The ring resonators were designed at University of Applied Sciences Wildau and fabricated in a 0.13 μm SiGe BiCMOS pilot line at IHP in Frankfurt (Oder), Germany using 200 mm silicon-on-insulator wafers and 248 nm DUV lithography. Three ring resonators with different slot widths ($s = 60$ nm, 120 nm, 150 nm) were realized. A scheme of typical ring resonator types including the partially slotted ring resonator is depicted in Figure 1. Conventional ring resonators are based on strip waveguides or slot waveguides, as depicted in Figure 1(a) and Figure 1(b), respectively. Strip-to-slot mode-converter are introduced in the bus waveguide in order to enhance the coupling efficiency in case of slot waveguide ring resonators (Figure 1(c)). In contrast to that the hybrid concept of the PSRR takes advantage of both a strongly guiding strip waveguide at the bent part and an efficient strip-loaded slot waveguide at the straight part of the oval shaped ring (racetrack configuration). A schematic of the PSRR is depicted in Figure 1(d). To exploit the advantages of each waveguide type an efficient strip-to-slot waveguide transition is needed. Therefore, we used a strip-to-slot mode-converter as depicted in Figure 1(d). The coupling distance and waveguide width are $d = 200$ nm and $w = 500$ nm, respectively. The length of the strip-loaded slot waveguide is $l = 12$ μm and the length of the strip-to-slot mode-converter is 8 μm. With the ring radius $R = 20$ μm and the coupling length $L = 28$ μm the total circumference results in $C = 182$ μm and a small foot print of 2.72 μm^2.

A detailed cross sectional view of the strip-loaded slot waveguide structure is shown in Figure 2. The strip-loaded slot waveguide consists of two silicon rails with a standard silicon-on-insulator height of $h_r = 220$ nm. All waveguides are located on top of a 2 μm buried oxide layer. The silicon strip-loads were etched remaining a silicon slab height of $h_l = 50$ nm and additionally n^+-implanted to decrease the electrical sheet resistance. In order to avoid excessive losses due to free carrier absorption the doping concentration was reduced close to the slot waveguide structure (n-implanted). The slot waveguide is electrically connected to Ground-Signal-Ground (GSG) aluminium electrodes through the doped silicon strip-loads and tungsten contacts (see Figure 2). In order to improve connectivity and conductivity a thin silicide intermediate layer was used to connect the tungsten contacts to the doped silicon to get an ohmic contact. Top view scanning-electron microscopic (SEM) images of the fabricated PSRR are shown in Figure 3. Figure 3(a) shows the GSG aluminium electrodes with a pitch of 150 μm and an impedance of 50 Ω. Figure 3(c) shows a cross-sectional view of the slot waveguide recorded with

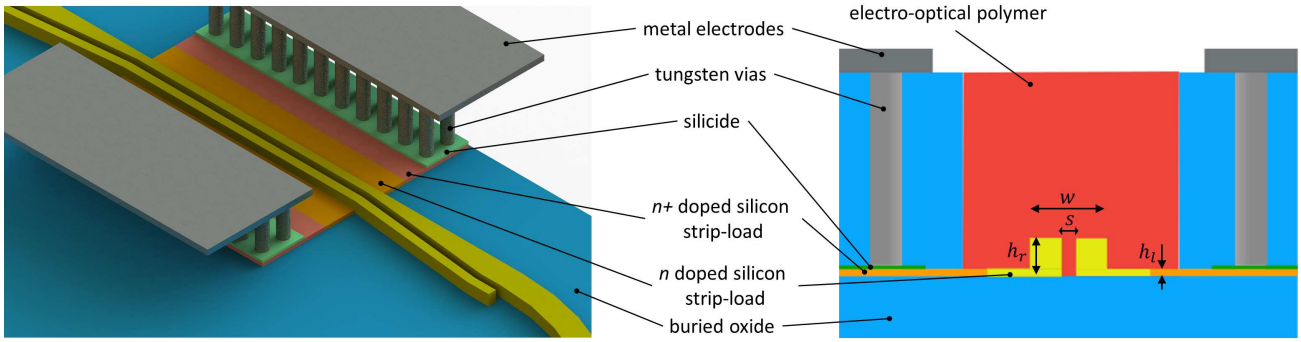

Figure 2. Detailed schematic of the strip-loaded slot waveguide part of the ring resonator and cross sectional diagram including electrical contacts (not to scale).

a focused ion beam (FIB).

A silicon dioxide top cladding is deposited and a trench is etched to open the slot waveguide structure as illustrated in Figure 2 and highlighted (blue) in Figure 3(a) and Figure 3(b). This allows the functionalization of the slot with an organic EO material.[9] Using EO polymers or organic crystals as cladding material the EO effect and therefore the device tunability is expected to be significantly higher compared to free-carrier plasma dispersion based phase shifters.[9,10] Further, the slot waveguide structure provides a high optical and electrical confinement which increases EO effects even more.[11,12]

As cladding material we have deposited a side-chain polymer system in a post-process. The polymer system consists of PMMA and the optical nonlinear chromophore Disperse Red 1 (DR1) (IUPAC Name: Poly[(methyl methacrylate)-co-(Disperse Red 1 acrylate)]). The chromophore concentration is nominally 25 mol%. As solvent we used 1,1,2,2-Tetrachloroethane. The resultant solution was filtered through a 0.2 μm PTFE membrane filter and spin-coated on the photonic chip at 6000 rpm. To ensure that the solvent was removed after spin-coating the photonic chips were heated on a hot plate in 10 °C steps from 30 °C to 60 °C for 2 h each step. This was followed by heating the chips to 80 °C for 10 h in a vacuum oven.

3. DEVICE CHARACTERIZATION

The transmission spectra of the fabricated device were obtained by a testing platform using a tunable external cavity laser (ECL) as light source with a bandwidth of < 1 pm and maximum output power of 14 dBm. The tuning range was between 1540 nm and 1580 nm in 1 pm steps. We used the ECL and a photodiode to measure the optical quality factor. For active measurements we employed a superluminescent diode as light source with a maximum output power of 10 dBm and an optical spectrum analyzer to obtain the transmission spectra. In both cases the light was coupled into the silicon waveguides through a fiber grating coupler and out-coupled through another grating coupler. Due to the polarization dependency of the grating coupler the polarization of the input light was controlled using a paddle style fiber polarization rotator in order to achieve TE-polarization. The photonic chip was measured on a temperature-controlled sample holder and stabilized to 35 °C using a hot plate in order to avoid changes in the transmission due to temperature fluctuation. For active measurements the GSG electrodes are connected to an electric power source through tungsten DC probes.

4. RESULTS AND DISCUSSION

4.1 DC device tunability

The DC device tunability was obtained by measuring the transmission at several DC voltages in a non-sequential fashion in order to exclude thermal drifts as the cause of the peak shifting behavior. An approximately linear wavelength shift was measured in the voltage range of 3 V to 7 V, as shown in Figure 4(a). The highest DC

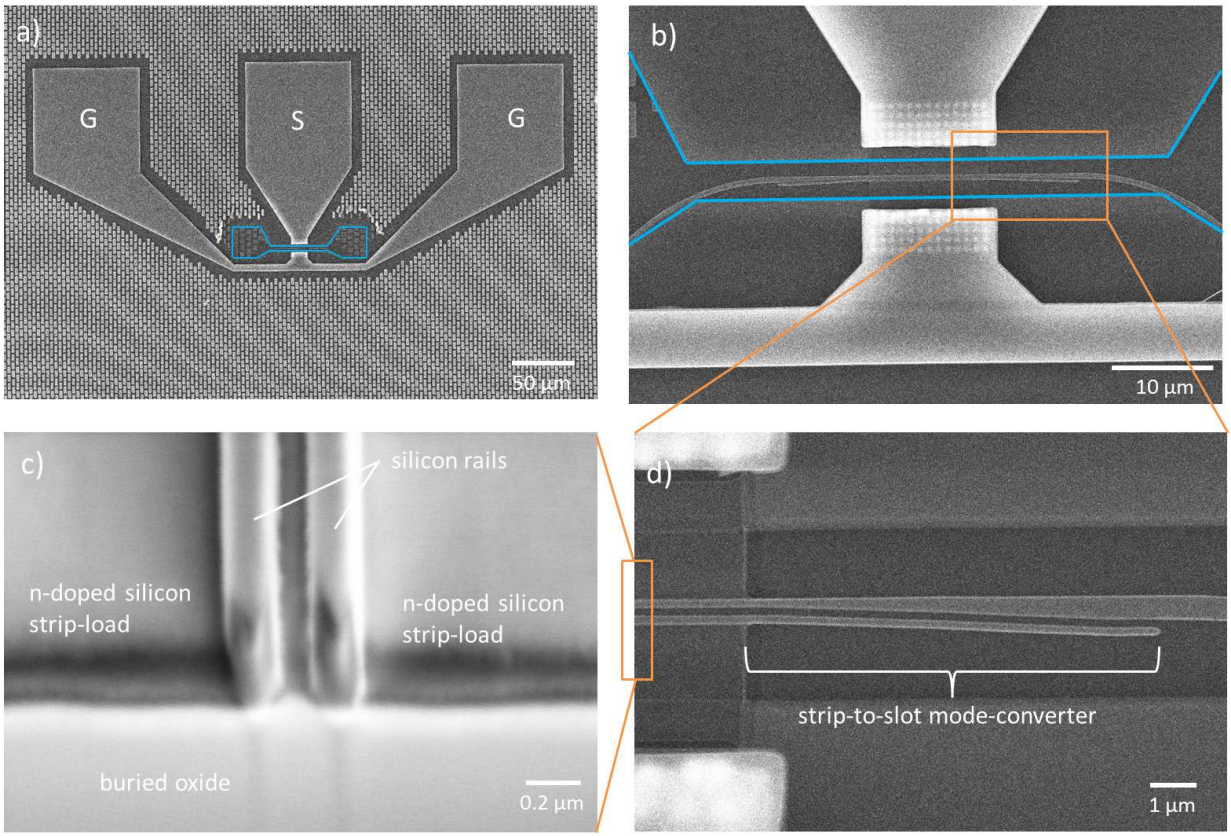

Figure 3. a) SEM image of the Ground-Signal-Ground (GSG) aluminium electrode from the top view with a trench (highlighted in blue) to functionalize the slot waveguide by an organic cladding material. b) SEM image of part of the ring resonator with strip-to-slot mode-converter and strip-loaded slot waveguide. c) FIB image of the strip-loaded slot waveguide. d) Magnification of the strip-to-slot mode-converter for the 150 nm slot waveguide.

device tunability of 707 pm/V has been achieved with the 110 nm slotted ring. With the narrow full width at half maximum of 15 pm and a corresponding optical quality factor of up to 10^5, as presented in our previous work,[8] this appears to be a convenient tuning range for most applications and offers the possibility for efficient on-off keying. Further, it should be highlighted that the achieved DC device tunability is more than 20 times higher compared to common ring-based modulators making use of the plasma dispersion effect.[13]

4.2 Poling efficiency

In order to compare our results with state-of-the-art silicon-organic hybrid devices we determined the poling efficiency which is the ratio between the linear EO coefficient and the applied poling field, r_{33}/E_{pol}.[9] The poling field is given by $E_{pol} = U/s$, where U is the applied voltage. With a linear regression we determined a poling efficiency of 0.31 $\mathrm{nm}^2/\mathrm{V}^2$ for the 110 nm and 150 nm slot waveguides as depicted in Figure 4(b). A poling efficiency of 0.09 $\mathrm{nm}^2/\mathrm{V}^2$ was obtained for the 60 nm slot waveguide. This small poling efficiency can be explained by a non-homogeneous infiltration of the narrow slot. However, our results are in good agreement with other publications were a guest-host polymer system consisting of PMMA and YLD124 was used and poling efficiency of 0.23 $\mathrm{nm}^2/\mathrm{V}^2$ is reported.[9] It should be mentioned that even higher poling efficiencies of about

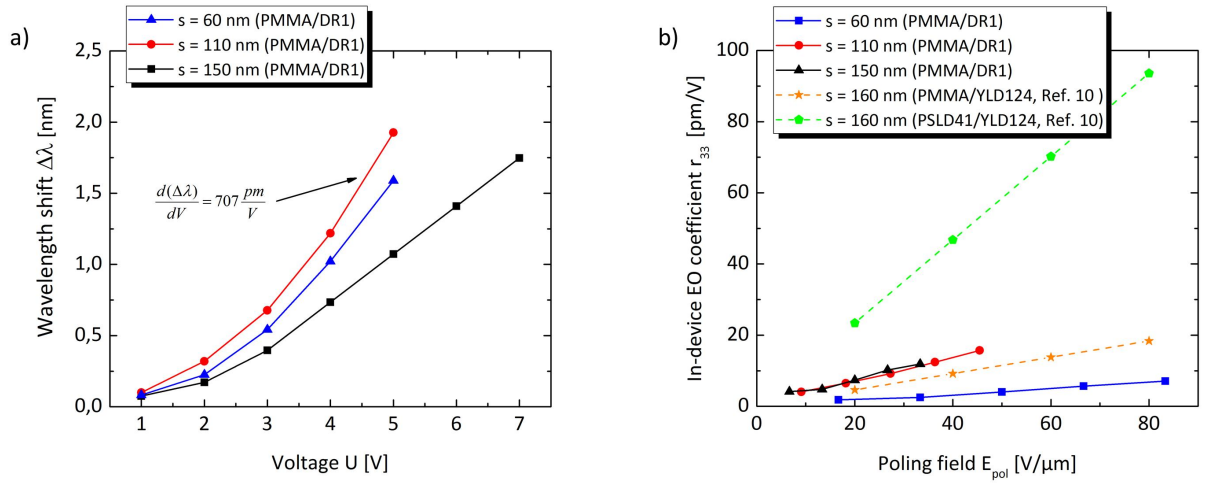

Figure 4. a) Voltage induced peak shift of the PSRR covered with PMMA/DR1. A maximum DC device tunability of 707 pm/V is obtained from the PSRR with a slot width of 110 nm. b) Linear EO coefficient as function of applied electric field for different slot widths (s). The slope of this lines are used to determine the poling efficiencies.

$0.92\,\mathrm{nm}^2/\mathrm{V}^2$ has been demonstrated recently with PSLD41 doped by 25 mol% YLD124 (binary chromophore organic glass).[9]

4.3 In-device linear EO coefficient

The most limiting factor of the presented PSRR is the EO polymer. We derive the in-device EO coefficient r_{33} assuming a phase shift $\Delta\phi = \Delta n \cdot k_0 \cdot l \cdot \Gamma_{slot}$ induced by the refractive index change $\Delta n = 1/2 \cdot n_{poly}^3 \cdot r_{33} \cdot E$. From the experimentally obtained wavelength shift the in in-device EO coefficient can be determined by

$$r_{33} = \frac{2 \cdot s \cdot \Delta\lambda}{n_{poly}^3 \cdot l \cdot U \cdot \Gamma_{slot}}, \tag{1}$$

where n_{poly} is the refractive index of the EO polymer and Γ_{slot} is the field confinement factor of the slot region.[14] The field confinement factor is usually defined as the ratio of the time averaged power flow in the slot area over the time averaged power flow in the total area.[15] Please note that in case of silicon-on-insulator slot waveguides a significant difference between the field confinement factor for the slot region and the whole cladding region exists.[12] The field confinement factor in the cladding region is about four times greater than in the slot region.[11] Here we use the slot region because the linear EO effect needs a non-centrosymmetrical orientation of the EO polymer. This is only guaranteed inside the slot because of the homogeneous electric field. For the slot width of 110 nm and a wavelength of $\lambda = 1550\,\mathrm{nm}$ the field confinement factor is $\Gamma_{slot} \approx 0.2$.[11] The in-device EO coefficient of the side-chain polymer system is determined to be $r_{33} = 12.8\,\mathrm{pm/V}$ assuming a voltage of $U = 1\,\mathrm{V}$ applied to the 110 nm wide slot waveguide with a wavelength shift of 707 pm. For comparison, the aforementioned binary chromophore organic glass (PSLD41/YLD124) exhibits a record-high in-device EO coefficient of $r_{33} = 230\,\mathrm{pm/V}$.[16] Using such advanced EO polymers the performance of the PSRR can be significantly improved.

5. CONCLUSION

In conclusion, we have demonstrated a PSRR covered with an EO polymer enabling the use of slot waveguide phase shifter while maintaining a high Q-factor and a small footprint. Under carefully controlled conditions we have experimentally shown a remarkable DC device tunability of 707 pm/V and a poling efficiency of

$0.31\ \mathrm{nm}^2/\mathrm{V}^2$ using a commercial side-chain Polymer (PMMA/DR1) with a moderate in-device EO coefficient of 12.8 pm/V. The PSRR appears to be promising for various fields of applications for integrated opto-electronics. In particular, the proposed design will be useful for integrated silicon-organic hybrid photonic devices such as optical switches, modulators, and tunable filters.

ACKNOWLEDGMENTS

We gratefully acknowledge the financial support provided by the German Federal Ministry of Education and Research (BMBF) under contract no. 03FH086PX2. We additionally thank P. Prosposito, F. De Matteis, and R. De Angelis from the University of Rome Tor Vergata, Italy, and A. Al-Saadi from the Technical University Berlin, Germany, for their encouragement. Furthermore, we thank J. Katzer, H. Silz, L. Zimmermann, B. Tillack, and A. Mai from the Institute of High-Performance Microelectronics (IHP), Germany for their support in the framework of the Joint-Lab IHP/TH Wildau.

REFERENCES

[1] Lauermann, M., Palmer, R., Koeber, S., Schindler, P. C., Korn, D., Wahlbrink, T., Bolten, J., Waldow, M., Elder, D. L., Dalton, L. R., Leuthold, J., Freude, W., and Koos, C., "Low-power silicon-organic hybrid (soh) modulators for advanced modulation formats," *Opt. Express* **22**, 29927–29936 (Dec 2014).

[2] Almeida, V. R., Xu, Q., Barrios, C. A., and Lipson, M., "Guiding and confining light in void nanostructure," *Opt. Lett.* **29**, 1209–1211 (Jun 2004).

[3] Leuthold, J., Koos, C., Freude, W., Alloatti, L., Palmer, R., Korn, D., Pfeifle, J., Lauermann, M., Dinu, R., Wehrli, S., Jazbinsek, M., Gunter, P., Waldow, M., Wahlbrink, T., Bolten, J., Kurz, H., Fournier, M., Fedeli, J.-M., Yu, H., and Bogaerts, W., "Silicon-organic hybrid electro-optical devices," *Selected Topics in Quantum Electronics, IEEE Journal of* **19**, 114–126 (Nov 2013).

[4] Baehr-Jones, T., Hochberg, M., Wang, G., Lawson, R., Liao, Y., Sullivan, P., Dalton, L., Jen, A., and Scherer, A., "Optical modulation and detection in slotted silicon waveguides," *Opt. Express* **13**, 5216–5226 (Jul 2005).

[5] Ding, R., Baehr-Jones, T., Kim, W.-J., Xiong, X., Bojko, R., Fedeli, J.-M., Fournier, M., and Hochberg, M., "Low-loss strip-loaded slot waveguides in silicon-on-insulator," *Opt. Express* **18**, 25061–25067 (Nov 2010).

[6] Gould, M., Baehr-Jones, T., Ding, R., Huang, S., Luo, J., Jen, A. K.-Y., Fedeli, J.-M., Fournier, M., and Hochberg, M., "Silicon-polymer hybrid slot waveguide ring-resonator modulator," *Opt. Express* **19**, 3952–3961 (Feb 2011).

[7] Claes, T., Molera, J., De Vos, K., Schachtb, E., Baets, R., and Bienstman, P., "Label-free biosensing with a slot-waveguide-based ring resonator in silicon on insulator," *Photonics Journal, IEEE* **1**, 197–204 (Sept 2009).

[8] Steglich, P., Mai, C., Stolarek, D., Lischke, S., Kupijai, S., Villringer, C., Pulwer, S., Heinrich, F., Bauer, J., Meister, S., Knoll, D., Casalboni, M., and Schrader, S., "Novel ring resonator combining strong field confinement with high optical quality factor," *Photonics Technology Letters, IEEE* **27**, 2197–2200 (Oct 2015).

[9] Palmer, R., Koeber, S., Elder, D. L., Woessner, M., Heni, W., Korn, D., Lauermann, M., Bogaerts, W., Dalton, L., Freude, W., Leuthold, J., and Koos, C., "High-speed, low drive-voltage silicon-organic hybrid modulator based on a binary-chromophore electro-optic material," *Journal of Lightwave Technology* **32**, 2726–2734 (Aug 2014).

[10] Korn, D., Jazbinsek, M., Palmer, R., Baier, M., Alloatti, L., Yu, H., Bogaerts, W., Lepage, G., Verheyen, P., Absil, P., Guenter, P., Koos, C., Freude, W., and Leuthold, J., "Electro-optic organic crystal silicon high-speed modulator," *Photonics Journal, IEEE* **6**, 1–9 (April 2014).

[11] Steglich, P., Villringer, C., Dümecke, S., Michel, Y. P., Casalboni, M., and Schrader, S., "Silicon-on-insulator slot-waveguide design trade-offs," in [*Proceedings of the 3rd International Conference on Photonics, Optics and Laser Technology*], 47–52 (2015).

[12] Steglich, P., Villringer, C., Dümecke, S., Michel, Y. P., Casalboni, M., and Schrader, S., "Design optimization of slot-waveguides covered with organic cladding materials for integrated photonic devices," in [*NWK 16*], Middendorf, S. and Hüttinger, G., eds., 192–198, BERLINER WISSENSCHAFTS-VERLAG GmbH (4 2015).

[13] Xuan, Z., Ma, Y., Liu, Y., Ding, R., Li, Y., Ophir, N., Lim, A. E.-J., Lo, G.-Q., Magill, P., Bergman, K., Baehr-Jones, T., and Hochberg, M., "Silicon microring modulator for 40 gb/s nrz-ook metro networks in o-band," *Opt. Express* **22**, 28284–28291 (Nov 2014).

[14] Chuang, S. L., [*Physics of Photonic Devices*], Wiley, 2 ed. (1 2009).

[15] Robinson, J. T., Preston, K., Painter, O., and Lipson, M., "First-principle derivation of gain in high-index-contrast waveguides," *Opt. Express* **16**, 16659–16669 (Oct 2008).

[16] Palmer, R., Koeber, S., Woessner, M., Elder, D. L., Heni, W., Korn, D., Yu, H., Lauermann, M., Bogaerts, W., Dalton, L. R., Freude, W., Leuthold, J., and Koos, C., "High-speed silicon-organic hybrid (soh) modulators with 230 pm/v electro-optic coefficient using advanced materials," in [*Optical Fiber Communication Conference*], *Optical Fiber Communication Conference* , M3G.4, Optical Society of America (2014).